TISSUE ENGINEERING: Part A
Volume 21, Numbers 1 and 2, 2015

DOI: 10.1089/ten.tea.2014.0095

Histologic Characterization of Acellular Dermal Matrices in a Porcine Model of Tissue Expander Breast Reconstruction

Christopher A. Carruthers, PhD,[1,2] Christopher L. Dearth, PhD,[2,3] Janet E. Reing, MS,[2] Caroline R. Kramer, BS,[2] Darcy H. Gagne, BS,[4] Peter M. Crapo, PhD,[4] Onelio Garcia, Jr., MD, FACS,[5] Amit Badhwar, PhD,[4] Jeffrey R. Scott, PhD,[4,6] and Stephen F. Badylak, DVM, PhD, MD[1–3]

Background: Acellular dermal matrices (ADMs) have been commonly used in expander-based breast reconstruction to provide inferolateral prosthesis coverage. Although the clinical performance of these biologic scaffold materials varies depending on a number of factors, an in-depth systematic characterization of the host response is yet to be performed. The present study evaluates the biochemical composition and structure of two ADMs, AlloDerm® Regenerative Tissue Matrix and AlloMax™ Surgical Graft, and provides a comprehensive spatiotemporal characterization in a porcine model of tissue expander breast reconstruction.
Methods: Each ADM was characterized with regard to thickness, permeability, donor nucleic acid content, (residual double-stranded DNA [dsDNA]), and growth factors (basic fibroblast growth factor [bFGF], vascular endothelial growth factor [VEGF], and transforming growth factor-beta 1 [TGF-β1]). Cytocompatibility was evaluated by *in vitro* cell culture on the ADMs. The host response was evaluated at 4 and 12 weeks at various locations within the ADMs using established metrics of the inflammatory and tissue remodeling response: cell infiltration, multinucleate giant cell formation, extent of ADM remodeling, and neovascularization.
Results: AlloMax incorporated more readily with surrounding host tissue as measured by earlier and greater cell infiltration, fewer foreign body giant cells, and faster remodeling of ADM. These findings correlated with the *in vitro* composition and cytocompatibility analysis, which showed AlloMax to more readily support *in vitro* cell growth.
Conclusions: AlloMax and AlloDerm demonstrated distinct remodeling characteristics in a porcine model of tissue expander breast reconstruction.

Introduction

Of the more than 91,000 breast reconstruction procedures in 2012, 70% involved a two-stage approach, in which an expander is placed below the pectoralis major and subsequently replaced with a permanent implant after the desired expansion is obtained.[1] The lower pole of the breast between the inferior edge of the pectoralis major and chest wall at the level of the inframammary fold is commonly bridged with an acellular dermal matrix (ADM).[2–6] The use of an ADM helps to shape the breast pocket and restore anatomic boundaries that may have been violated during the mastectomy, aids in preventing superior migration of the pectoralis major or tissue expander during expansion, allows for more intraoperative expansion and thus typically requires fewer office visits for postoperative expansion, provides an extra layer of coverage over the lower pole of the tissue expander, facilitates the use of single-stage breast reconstruction, and protects the expander in the lower pole from exposure in complicated mastectomies (e.g., dehiscence).[7]

ADMs are derived from the extracellular matrix (ECM) of dermal tissue. The ECM represents the secreted products of resident cells and has been shown to provide cues that affect cell migration, proliferation, and differentiation.[8–13] Thus, ECM scaffolds have the potential to act as an inductive template for the *in situ* formation of site-specific functional host tissue.[14,15] ECM scaffolds have been harvested from a variety of tissues and organs[16–26] and have been used in a broad range of clinical applications,[27–35]

[1]Department of Bioengineering, University of Pittsburgh, Pittsburgh, Pennsylvania.
[2]McGowan Institute for Regenerative Medicine, University of Pittsburgh, Pittsburgh, Pennsylvania.
[3]Department of Surgery, University of Pittsburgh, Pittsburgh, Pennsylvania.
[4]C. R. Bard, Inc. (Davol), Providence, Rhode Island.
[5]Division of Plastic Surgery, Miller School of Medicine, University of Miami, Miami, Florida.
[6]Department of Molecular Pharmacology, Physiology and Biotechnology, Brown University, Providence, Rhode Island.

including breast reconstruction.[2–6] The source tissue from which ECM scaffolds are manufactured has been shown to contain specific biologic cues that can affect the host remodeling response.[21–25,36–39] Preservation of the complex composition and three-dimensional ultrastructure of the ECM during manufacturing of these grafts is highly desirable, but it is recognized that all methods of tissue decellularization result in some degree of disruption of the architecture with potential loss of surface structure and composition.[14] For example, when the processing methods do not effectively decellularize the source tissue or when chemicals are involved that create nondegradable molecular crosslinks, the *in vivo* soft tissue remodeling response has been associated with chronic inflammation, fibrotic encapsulation, and scar tissue formation.[13,40,41] With the expanding list of available biologic scaffold materials for soft tissue reconstruction, all of which differ in source tissue and/or method of processing, a thorough understanding of the factors that affect the host response is necessary to select the most appropriate biologic scaffold for each clinical application. The aim of the present study was to compare the composition, structure, and *in vivo* host tissue response of two commercially available human ADMs, AlloDerm® Regenerative Tissue Matrix and AlloMax™ Surgical Graft, in a porcine model of tissue expander breast reconstruction. Evaluation criteria included biochemical composition and cytocompatibility *in vitro*, and established quantitative histomorphologic metrics that include recognizable aspects of the inflammatory and tissue remodeling responses *in vivo*.[42,43]

Materials and Methods

In vitro *material properties*

The thickness of each nonimplanted ADM was measured at 10 evenly spaced locations along each sample (3 different lots of each material and 10 samples per lot for a total of 300 measurements per ADM). Measurements were performed using a digital micrometer before and after hydration.

The hydrostatic permeability index (i.e., porosity index; defined as mL/cm^2/min under 120 mmHg pressure) of each material was measured, as previously described.[44] In brief, a hydrostatic pressure head of 120 mmHg was applied using water over a specified area and time frame, and the volume of water that passed through the specimen was measured. The test was performed on material from 3 different lots of production, with 10 samples per lot for a total of 30 tests for each ADM.

In vitro *composition analysis*

The degree of decellularization was assessed for three lots of AlloDerm Regenerative Tissue Matrix (AlloDerm; LifeCell Corp., Branchburg, NJ) and three lots of AlloMax Surgical Graft [AlloMax; C. R. Bard, Inc. (Davol), Warwick, RI] by three previously established criteria[14]: (i) the presence or absence of intact cells and nuclei on hematoxylin and eosin (H&E)-stained sections and 4′,6-diamidino-2-phenylindole (DAPI)-stained sections, respectively; (ii) the Quant-iT PicoGreen assay (Invitrogen, Carlsbad, CA) for quantification of double-stranded DNA (dsDNA); and (iii) evaluation of samples by agarose gel (2%) electrophoresis to determine the size of remaining DNA fragments.

Growth factors and total protein content were measured for three lots of AlloDerm and three lots of AlloMax. Concentrations of basic fibroblast growth factor (bFGF), vascular endothelial growth factor (VEGF), and transforming growth factor-beta 1 (TGF-β1) in urea–heparin extracts of dermis samples (see Reing *et al.*[45] for further detail of urea–heparin extract preparation) were determined using the Quantikine Human FGF basic Immunoassay, Human VEGF Immunoassay, and Mouse/Rat/Porcine/Canine TGF-β1 Immunoassay (all R&D Systems, Minneapolis, MN) according to the manufacturer's protocols. bFGF and VEGF assays were performed in duplicate; TGF-β1 assay was performed in triplicate. Growth factor assays measured the growth factor concentration and did not measure the growth factor activity. The concentration of total protein in the urea–heparin extracts was determined by the bicinchoninic acid (BCA) Protein Assay (Pierce, Rockford, IL) following the manufacturer's protocol.

In vitro *cytocompatibility analysis*

NIH 3T3 mouse fibroblast cells (American Type Culture Collection [ATCC] #CRL-1658, Manassas, VA) were grown in Dulbecco's modified Eagle's medium supplemented with 10% fetal bovine serum, 100 U/mL penicillin, and 100 μg/mL streptomycin; human microvascular endothelial cells (HMECs) (a gift from Francisco Candal, Center for Disease Control and Prevention, Atlanta, GA) were cultivated in the MCDB-131 medium containing 10% fetal bovine serum, 2 mM L-glutamine, 100 U/mL penicillin, and 100 μg/mL streptomycin. The MCDB-131 medium was from Invitrogen; all other reagents for cell growth were from Thermo Fisher Hyclone (Logan, UT). Cells were grown at 37°C in 5% CO_2/95% air and harvested for seeding when they were ~90–95% confluent. Grafts were cut to 2.5 cm^2 pieces, placed in six-well cell culture dishes, hydrated as per manufacturer's instruction for use protocol, and then incubated in the appropriate cell growth media at 37°C and 5% CO_2 for 15 min before cell seeding. The media were removed from the wells, stainless steel rings with inner diameters of 1.5 cm^2 were placed on the grafts, and cells were seeded on the grafts within the rings at 10^6 cells/1.5 cm^2. Each cell type was seeded on two lots of AlloDerm and two lots of AlloMax. For each lot of material, each cell type was seeded on each side of the graft in triplicate resulting in a total of six samples per lot seeded with each cell type. After a 7-day incubation, the cell culture media were removed, and the grafts with attached cells were immediately fixed in 10% neutral buffered formalin for 18 h. Following fixation, the samples were paraffin embedded, sectioned, and mounted on glass slides. Slides were stained with H&E, representative microscopic images captured, and images scored for cell confluence on the dermis substrate, cell phenotype, and cell infiltration into the dermis substrate using a standardized quantitative scaling system.[45,46] Descriptions of these metrics can be found in Table 1. Images were scored on a scale of 0–100 for each metric by five individuals who were blinded with respect to the identity of the samples, and an average score for each image was determined.

Surgical procedure

A recently described porcine model of bilateral breast reconstruction was used to evaluate ADM materials *in vivo*.[47]

Table 1. Descriptions of the Metrics Used for Semiquantitative Scoring of 3T3 Fibroblasts and Human Microvascular Endothelial Cells[46]

Metric	*Description*
Confluence (%)	The confluence score is defined as the percentage of the surface covered with cells. A score of 100 would indicate a fully coated surface with adjoining cells and no gaps.
Infiltration (%)	The infiltration score is defined as the percentage of the total depth, in which cells have migrated within the tissue. For example, if cells are found halfway into the tissue, this would correspond to an infiltration score of 50.
Phenotype (%)	They phenotype score is defined as the percentage of healthy appearing cells. A healthy cell is flat and fully adhered to surrounding tissue and other cells. An unhealthy is round and not adhered to the surrounding tissue or other cells.

The surgical procedures were conducted at DaVINCI Biomedical Research Products, Inc. (South Lancaster, MA) after protocol approval by the Institutional Animal Care and Use Committee. Twenty-one female Yorkshire Pigs (*Sus scrofa domesticus*, 46.2 ± 4.4 kg) were randomized into groups receiving bilaterally implanted tissue expanders (6×16 cm) consisting of either AlloDerm or AlloMax. The implants were explanted at 4 or 12 weeks ($n = 9$–10 implants per group per time point). One AlloDerm implant and two AlloMax implants had to be excluded due to host-inflicted damage to the implant site unrelated to graft performance. Animal care and surgical procedures followed the previously described protocol[47] exactly except for an important clinically relevant modification. In the present study, the tissue expanders were filled immediately upon implant and again at 2 weeks postsurgery rather than upon implant only.

In brief, the procedure consisted of intravenous administration of prophylactic antibiotic (ceftiofur, 5 mg/kg), intramuscular sedation [ketamine (20 mg/kg), xylazine (2 mg/kg), and atropine (0.04 mg/kg)], intubation, and surgical site preparation of the ventral and lateral thoracic regions, followed by induction of surgical plane anesthesia (isoflurane). A subcutaneous subpectoral pocket simulating a postmastectomy defect was created on one side of the thoracic region using a diagonal skin incision rostral to the mammary glands followed by diagonal dissection of the pectoralis major near its origin. All diagonal dissections were rostromedial to caudolateral. An ADM was rehydrated as per the manufacturer's instructions and sutured along the defect's caudomedial aspect to define simulated lateral mammary and inframammary folds. A deflated tissue expander (Siltex® Contour Profile® CPX3™ Low Height 250 mL; Mentor Worldwide LLC, Santa Barbara, CA) soaked in a triple antibiotic solution (>5 min in saline with cefazolin, gentamicin, and bacitracin) was then placed within the submuscular pocket and anchored through its suture tabs. The tissue expander was partially filled (~ 175 mL saline), and the ADM was trimmed and sutured to the pectoralis in a bridging position to fully cover the exposed portion of the expander. Anesthetic and antibiotic (bupivacaine and either cefotaxime or cefazolin) were applied to the wound interior and the skin flap was reapproximated and closed subcutaneously with subcuticular reinforcement. A symmetrical procedure was performed on the animals' opposite side using the same ADM type. The expanders were promptly filled transcutaneously to place mild tension on the skin flaps as assessed by palpation. Upon skin closure, the thoracic portion of each animal was wrapped to protect implant sites. Following recovery, animals were provided food and water *ad libitum* throughout the implant duration. At 2 weeks postsurgery, animals were anesthetized and expanders received an additional volume of saline without occluding blood flow to the overlying skin flaps. This procedure mimics the initial steps of breast reconstruction following mastectomy. Euthanasia at either 4 or 12 weeks postimplantation was achieved by intravenous sodium pentobarbital in accordance with the American Veterinary Medical Association (AVMA) Guidelines on euthanasia.

Explant histomorphometry

Following explantation of the tissue expander and adjacent tissues, histologic sections were prepared from three distinct anatomic locations that included the (i) midsubstance of the ADM material, the (ii) ADM-pectoralis muscle interface, and the (iii) ADM-chest wall interface. Each of these histologic sections traversed the dermis, ADM, and tissue expander interface. Sections were stained with H&E to assess cell infiltration, multinucleate giant cell formation, amount of remodeled ADM material, and the thickness of the interface tissue layer between the ADM and tissue expander. Von Willebrand Factor (vWF) immunolabeling was used to quantify neovascularization within the ADM. All of these characteristics were evaluated quantitatively by blinded scorers using detailed instructions[42,43] both within the ADM and at the ADM-tissue expander interface for each of the three anatomic locations. The morphologic appearance of the ADM material was readily distinguishable from newly deposited connective tissue accumulated as a consequence of host remodeling. A subjective estimate of the amount of remodeled ADM material could be made, thus providing a qualitative assessment of the amount of remaining scaffold material at each time point. With two time points, three animals per time point, two ADM materials, bilateral implants, three explant locations (e.g., ADM midsubstance, ADM-pectoralis muscle interface, and ADM-chest wall interface), and three images per interface, the number of images per stain generated was 216.

Statistics

Histologic analysis was performed with a two-way ANOVA with independent variables of time and ADM, location and ADM, or interface and ADM, followed by a *post hoc* Tukey test. A bivariate correlation was performed to compute Pearson's correlation coefficient across all dependent variables to quantitatively identify significant relationships between scaffold composition and host remodeling response.

Table 2. *In Vitro* Analysis of Extracellular Matrix Scaffolds

Metric	*AlloDerm®*	*AlloMax™*
Porosity (mL/cm^2/min)[a]	0.03 ± 0.16	1.30 ± 2.90
Dry thickness (mm)[a]	1.99 ± 0.29	1.30 ± 0.17
Wet thickness (mm)[a]	2.10 ± 0.26	1.82 ± 0.26
Protein (mg/g dry weight)[a]	9.90 ± 2.74	28.64 ± 7.74
bFGF (pg/g dry weight)[a]	8545 ± 1135	0.00 ± 30
VEGF (pg/g dry weight)[a]	4068 ± 2181	392 ± 449
TGF-β1 (pg/g dry weight)	392 ± 434	0.00 ± 93

Mean ± standard deviation.
[a]$p < 0.05$.
bFGF, basic fibroblast growth factor; TGF-β1, transforming growth factor-beta 1; VEGF, vascular endothelial growth factor.

Results

ADM biochemical and physical properties

The biochemical and physical properties of AlloDerm and AlloMax were quantified. The porosity index of AlloDerm and AlloMax was found to be strikingly different with values of 0.03 and 1.30, respectively (Table 2). AlloDerm was found to be thicker, both dry and when rehydrated, than AlloMax (Table 2). AlloMax contained more soluble protein than AlloDerm (Table 2). Growth factor analysis shows that AlloDerm contained more bFGF and VEGF than AlloMax (Table 2).

Decellularization evaluation

The extent of decellularization for both AlloDerm and AlloMax was evaluated by established metrics.[14] H&E- and DAPI-stained sections show that AlloDerm contains intact cells, whereas only cell remnants were found within AlloMax (Fig. 1A, B). Furthermore, both ADMs contain large DNA (>1500 bp) fragments as evaluated by agarose gel electrophoresis (Fig. 1C). dsDNA quantification of the ADMs showed that while both materials contained measurable amounts of dsDNA, AlloMax (200 ± 12 ng dsDNA/mg dry weight) contained lower amounts compared to AlloDerm (1671 ± 251 ng dsDNA/mg dry weight) (Fig. 1D). Overall, AlloMax was found to be more thoroughly decellularized than AlloDerm.

Cytocompatibility

The ability of the ADMs to support cell growth *in vitro* was assessed by established quantitative metrics of cell confluence, cell phenotype, and cell infiltration using two distinct cell lines—NIH 3T3 mouse fibroblast cells and HMECs.[45,46] Fibroblasts showed 30% higher scores for growth on AlloDerm compared to AlloMax (Fig. 2A, B). HMECs showed a 92% higher cytocompatibility score on AlloMax compared to AlloDerm, primarily as a result of superior confluence and phenotype scores (Fig. 2C, D). The stark contrast in the ability of each ADM to support HMEC growth is clearly evident in Figure 2C.

Characterization of the in vivo *host remodeling response*

A porcine model of bilateral breast reconstruction was used to evaluate each ADM material *in vivo*. The *in vivo* host remodeling response was characterized by established quantitative histomorphologic metrics as a function of time and location within the explant.

Cellularity within the ADM increased as a function of time for both materials (Fig. 3C). At 12 weeks, AlloMax had 25% greater cellularity than AlloDerm (Fig. 3B, C) particularly at both the ADM pectoralis interface and ADM-chest wall interface (Fig. 3D). Cells were found to be uniformly distributed along the length of each graft (e.g., at the ADM-pectoralis interface, ADM-chest wall interface, and throughout the ADM between the two interfaces; see Fig. 3D). Multinucleate giant cell formation within the AlloDerm material increased as a function of time and was greater

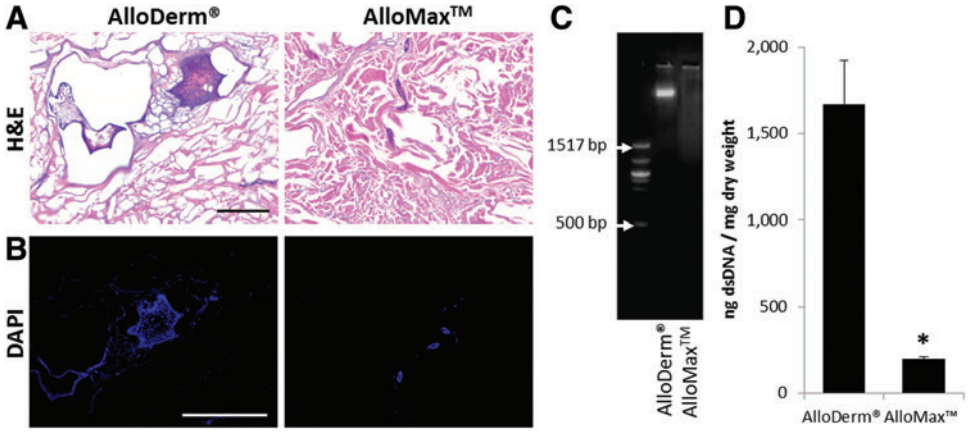

FIG. 1. Decellularization assessment before implantation. **(A)** Hematoxylin and eosin (H&E) staining to probe for intact cells (scale bar represents 100 μm), where the nuclei of cells stain blue if present and tissue and acellular dermal matrix (ADM) stain pink. **(B)** 4′,6-Diamidino-2-phenylindole (DAPI) staining to probe for intact nuclei (scale bar represents 50 μm). **(C)** Ethidium bromide gel to inspect base-pair size of remnant double-stranded DNA (dsDNA). **(D)** PicoGreen assay to quantify dsDNA. Both ADMs contained remnants of cells with AlloDerm® Regenerative Tissue Matrix and significantly greater amounts of DNA than AlloMax™ Surgical Graft. Significant difference ($p < 0.05$) is denoted by (*). Color images available online at www.liebertpub.com/tea

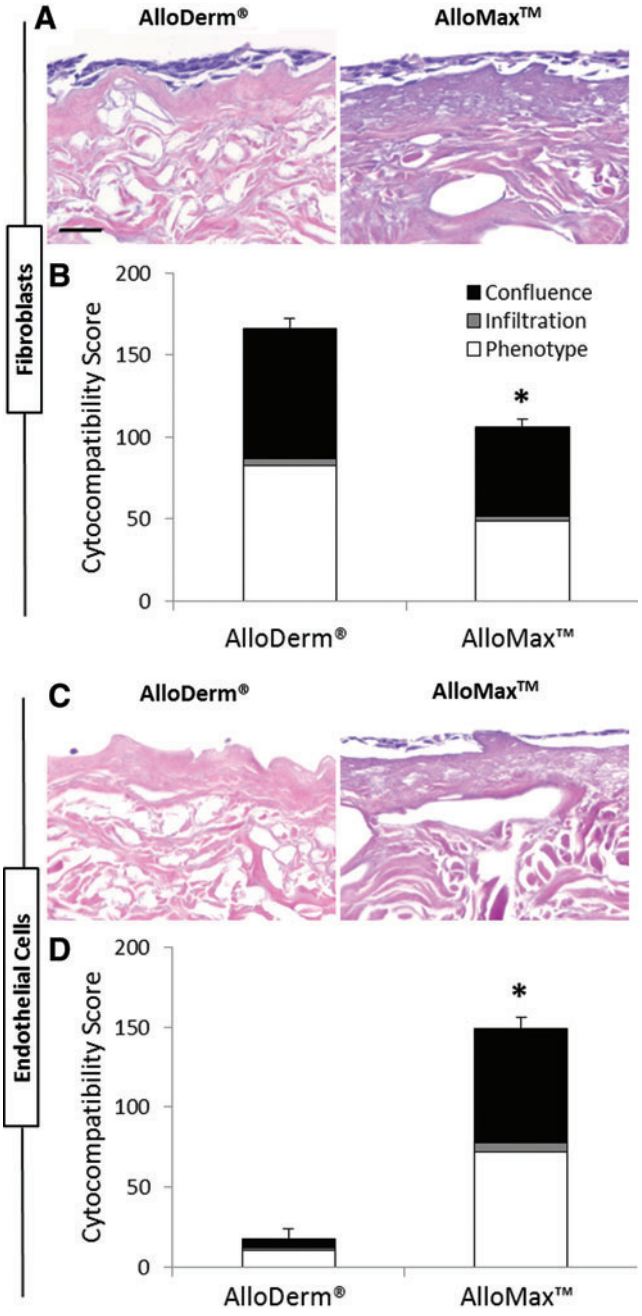

FIG. 2. *In vitro* cytocompatibility assessment. **(A, B)** NIH 3T3 fibroblasts and **(C, D)** human microvascular endothelial cells (HMECs) were seeded in triplicate on each side of the grafts for two lots of AlloDerm and two lots of AlloMax and cultured for 7 days. H&E images **(A, C)** were subsequently scored for confluence, phenotype, and infiltration **(B, D)**. AlloDerm was more cytocompatible than AlloMax for fibroblasts, and AlloMax was more cytocompatible than AlloDerm for endothelial cells. Significant differences ($p < 0.05$) are denoted by (*). Scale bar represents 50 μm. Color images available online at www.liebertpub.com/tea

compared to AlloMax at both 4 and 12 weeks (Fig. 4B); particularly at the ADM-pectoralis interface (Fig. 4C). Cells staining positive for vWF, a marker expressed by endothelial cells and relevant to neovascularization, increased from 4 to 12 weeks and were similar in magnitude for both ADMs (Fig. 5B). At 12 weeks, there was a twofold greater amount of vWF-positive staining cells for AlloMax at the ADM-chest wall interface compared to the ADM-pectoralis interface and throughout the ADM (Fig. 5C). For AlloDerm, cells were found to be uniformly distributed within the graft (Fig. 5C).

The extent of ADM remodeling increased for both materials over time; however, AlloMax was significantly more remodeled than AlloDerm at both time points (Fig. 6B). Specifically, AlloDerm was found to be ~30% and 50% remodeled following 4 and 12 weeks, respectively, whereas AlloMax was found to be ~50% and 80% remodeled at the same time points (Fig. 6B). When examined as a function of location at 12 weeks, AlloMax was found to be more remodeled along the length of the entire graft compared to AlloDerm (Fig. 6C), with the highest remodeling score occurring at the ADM-chest wall interface (Fig. 6C).

Greater ADM remodeling of AlloMax was consistent with increased cellular infiltration, with a Pearson's correlation coefficient of $r = 0.933$ ($p = 0.007$). Strong correlations were also observed between remodeling and residual DNA (Pearson's correlation coefficient of $r = -0.921$; $p = 0.009$) and between cell infiltration and residual DNA (Pearson's correlation coefficient of $r = -0.842$; $p = 0.036$).

Discussion

ECM scaffold materials, including ADMs, are harvested by decellularization of a variety of allogeneic or xenogeneic tissues and organs. The resultant acellular ECM scaffolds are composed of a tissue-specific 3D architecture and composition of structural and functional molecules produced by the resident cells. ECM scaffolds have been shown to contain biologic cues that can affect the host remodeling response, including cell migration, proliferation, and differentiation and thus have the potential to act as an inductive template for the *in situ* formation of site-specific functional host tissue.[24,25,36–39] Indeed, various ECM scaffolds have been used in a broad range of preclinical and clinical applications, including breast reconstruction.[2–6,15,31–35,48–55]

Of the nearly 100,000 mastectomy-related breast reconstruction procedures conducted each year, ~70% involve an immediate, staged breast reconstruction procedure, in which an initial tissue expander is subsequently replaced by a permanent implant. A major challenge associated with this procedure is achieving sufficient coverage of the lower pole of the breast to bridge the gap between the inferior edge of the pectoralis major and chest wall and thus prevent inferior migration of the expander/implant. To address this need, ADMs have been used during staged breast reconstruction procedures as a supporting bioscaffold. The ADMs also improve cosmetic outcomes by allowing surgeons to define the shape/contour of the breast pocket; preventing migration of the pectoralis major or tissue expander during expansion; and providing an extra layer of coverage over the lower pole of the tissue expander.

Despite the increasing use of ADMs in breast reconstruction procedures, limited information is available regarding the tissue and scaffold remodeling events that occur following implantation. The present study provides a quantitative and comprehensive spatiotemporal characterization of two commercially available human ADMs, AlloDerm

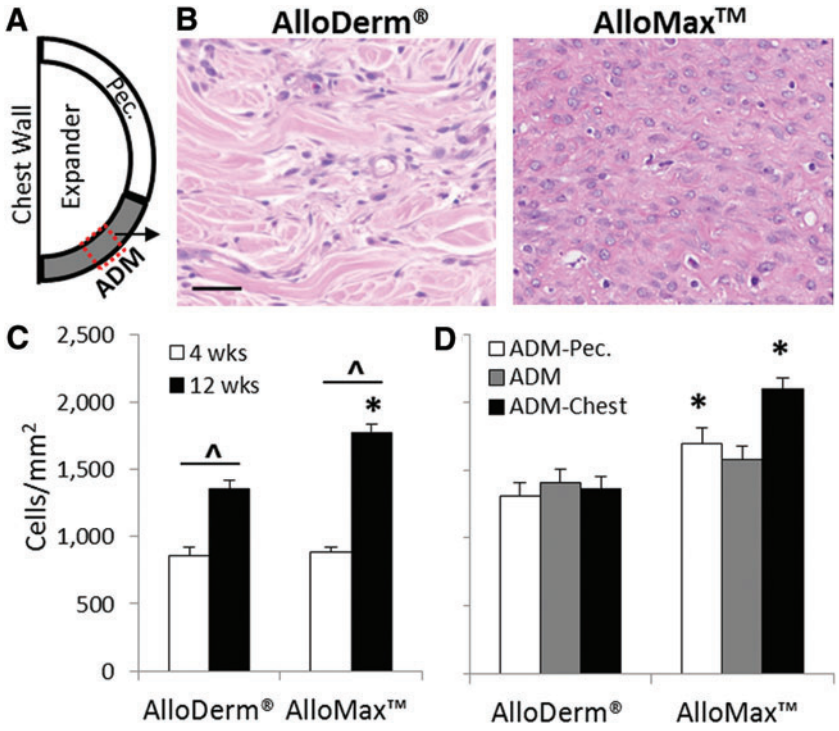

FIG. 3. Cell infiltration. **(A)** Depiction of ADM implants connecting pectoralis muscle (pec.) to the chest wall. **(B)** Representative H&E images of AlloDerm and AlloMax at 12 weeks postimplantation. Cell count as a function of **(C)** time, and at 12 weeks as a function of **(D)** location. Higher cellular infiltration was seen in AlloMax compared to AlloDerm. Significant differences ($p < 0.05$) are denoted by (*) AlloMax greater than AlloDerm; (^) different within AlloDerm or AlloMax. Scale bar represents 50 µm. Color images available online at www.liebertpub.com/tea

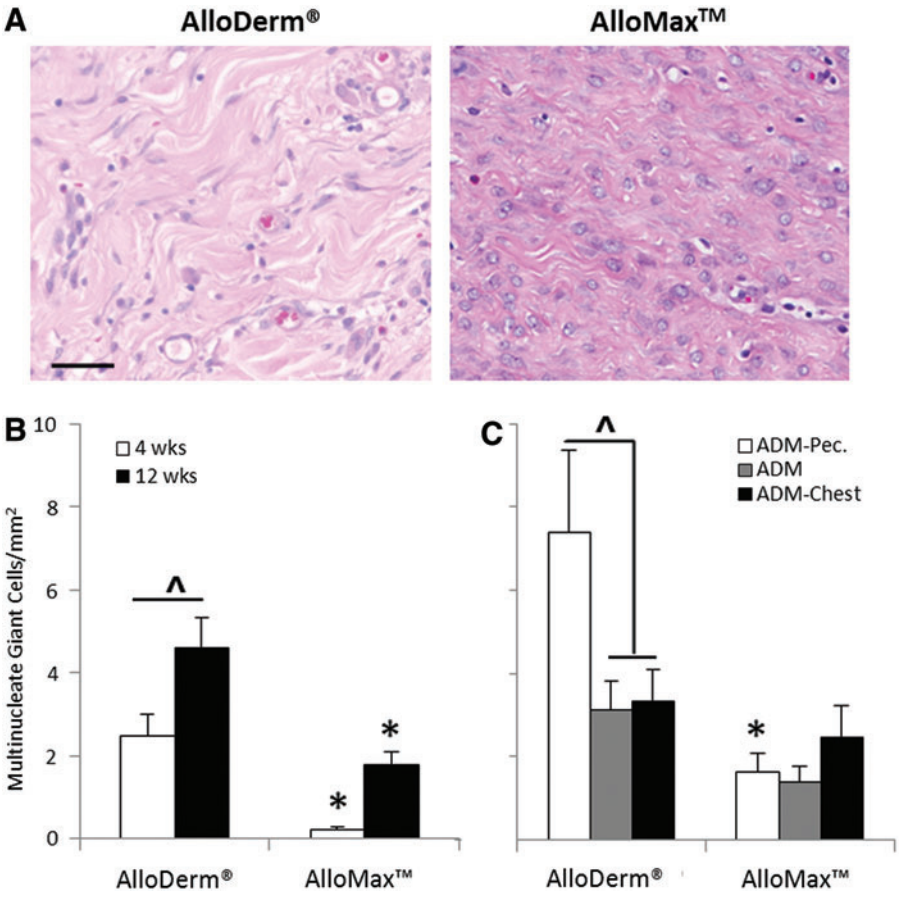

FIG. 4. Multinucleated giant cell formation. **(A)** Representative H&E images of AlloDerm and AlloMax at 12 weeks postimplantation. Multinucleated giant cell count as a function of **(B)** time, and at 12 weeks as a function of **(C)** location. AlloMax had fewer multinucleated giant cells present compared to AlloDerm. Significant differences ($p < 0.05$) are denoted by (*) less than AlloDerm (^), different within AlloDerm or AlloMax. Scale bar represents 50 µm. Color images available online at www.liebertpub.com/tea

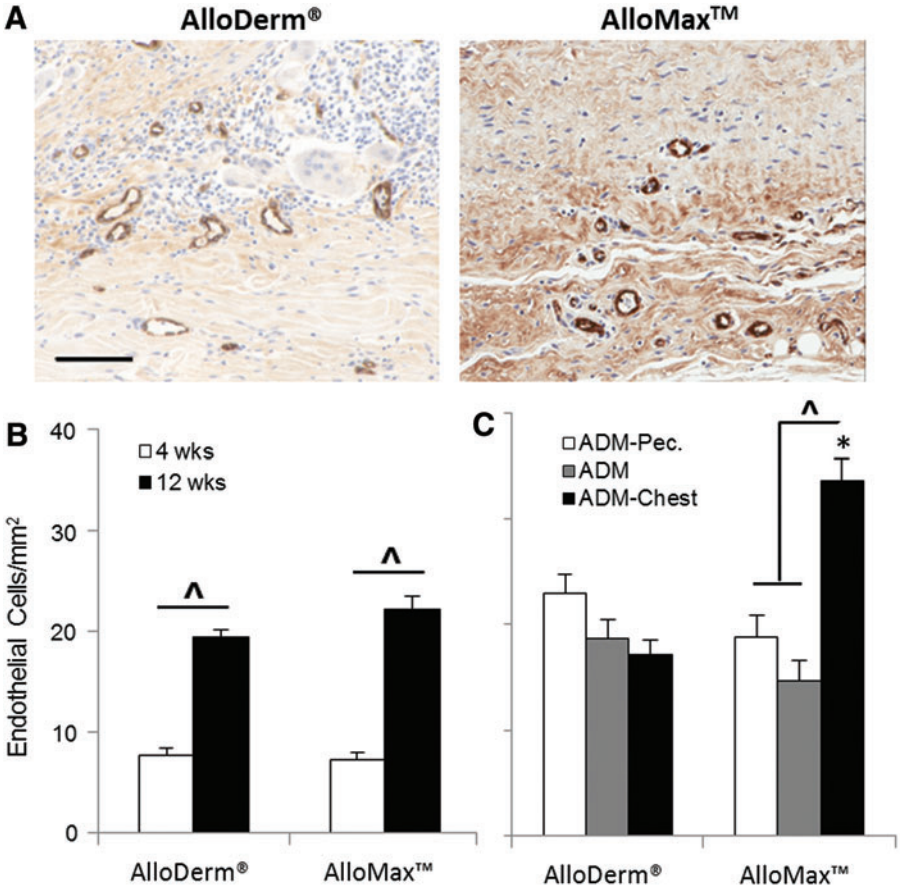

FIG. 5. Neovascularization. **(A)** Representative von Willebrand Factor (vWF) images of AlloDerm and AlloMax at 12 weeks within the center of the ADM. vWF-positive cells as a function of **(B)** time, and at 12 weeks as a function of **(C)** location. Both ADMs had an increase in vascularization with time as indicated by vWF staining of endothelial cells. Significant differences ($p < 0.05$) are denoted by (*) greater than AlloDerm (^), different within AlloDerm or AlloMax. Scale bar represents 100 μm. Color images available online at www.liebertpub.com/tea

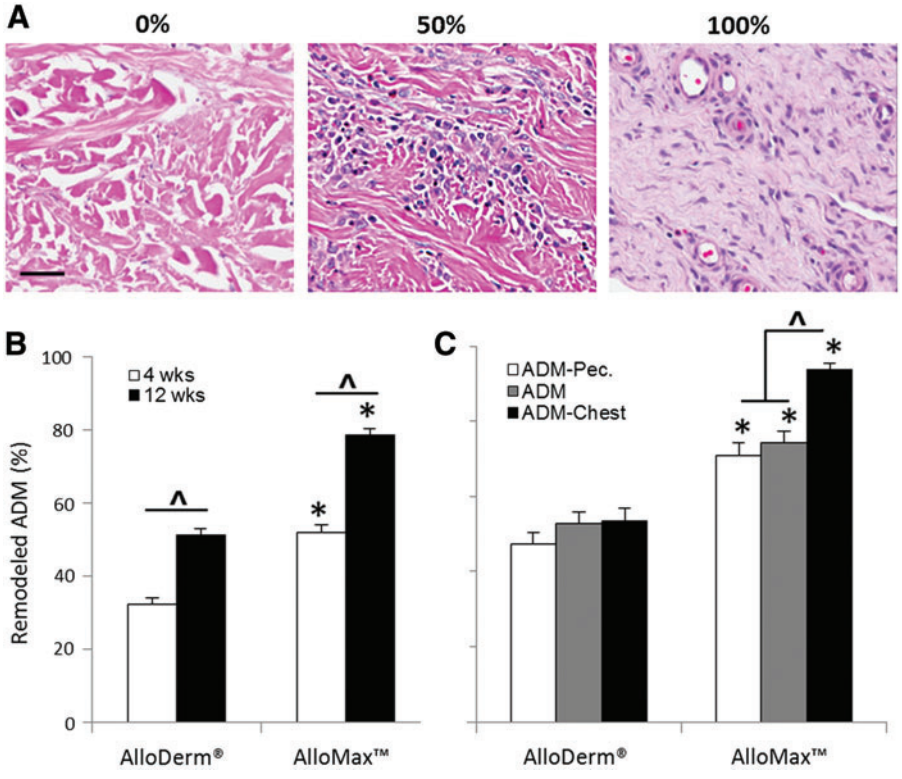

FIG. 6. ADM remodeling. **(A)** Representative H&E images of AlloDerm and AlloMax at 12 weeks postimplantation within the ADM. ADM remodeling as a function of **(B)** time, and at 12 weeks as a function of **(C)** location. AlloMax had more extensive graft remodeling compared to AlloDerm. Significant differences ($p < 0.05$) are denoted by (*) greater than AlloDerm (^), different within AlloDerm or AlloMax. Scale bar represents 50 μm. Color images available online at www.liebertpub.com/tea

Regenerative Tissue Matrix and AlloMax Surgical Graft, both *in vitro* and in a preclinical large animal model of tissue expander breast reconstruction. A recently described porcine model of breast reconstruction[47] was used to provide a histomorphologic analysis platform and characterize key elements of the *in vivo* host remodeling response by quantitative metrics in a controlled spatiotemporal manner. Two time points, 4 and 12 weeks postimplantation, were chosen to evaluate both the acute and chronic host tissue remodeling responses, respectively. Additionally, the host response was evaluated at various locations within the explanted tissue [i.e. (i) midsubstance of the ADM material, (ii) the ADM-pectoralis muscle interface, and (iii) the ADM-chest wall interface], which provided a comprehensive assessment of histomorphologic changes.

Although both AlloDerm and AlloMax are derived from the same starting material, human dermis, the biochemical composition, ability to support cell growth *in vitro*, and *in vivo* remodeling response of each material were distinct. For example, the *in vitro* composition and cytocompatibility analysis found AlloMax to be more thoroughly decellularized and to support the growth of HMECs *in vitro* than AlloDerm. *In vivo*, AlloMax incorporated more readily with surrounding host tissue as measured by the earlier and greater cell infiltration, fewer foreign body giant cells, and faster remodeling kinetics. Key differences in composition and cytocompatibility were found to be strongly correlated with the *in vivo* host response to these ADMs. While the cause of these divergent results is likely multifactorial, variations in the processing methods used during the manufacturing of ADMs are known to be critically important to both the material properties and resultant host response.[45,46]

A wide array of protocols have been described for the manufacturing (i.e., decellularization, terminal sterilization) of ECM scaffold materials derived from numerous tissues and organs. The main goals of all of these manufacturing protocols are the same: removal of as much of the cellular components of the source tissue as possible while simultaneously preserving the native composition and 3D ultrastructure of the ECM. Whereas it is recognized that all manufacturing protocols have limitations and result in some degree of deleterious change in the matrix composition and ultrastructure, the extent to which they affect the material properties and host response varies. For example, the type and sequence of detergents used can cause marked changes in growth factor and glycosaminoglycan content, mechanical strength, remodeling rate, and/or cytocompatibility of the biologic scaffold materials.[45,56–58] It is known that insufficient removal of cells or cell remnants from the source tissue or the introduction of chemicals that create nondegradable molecular crosslinks elicits a chronic proinflammatory host response, fibrotic encapsulation, and scar tissue formation.[13,40,41] Thus, it is plausible and logical that the disparate host response to AlloDerm and AlloMax could be due, at least in part, to differences in decellularization (i.e., the amount of cellular debris remaining) and/or changes in the composition and structure. However, the manufacturing processes of both materials tested herein are proprietary and identification of the key variables that drive this response is not possible.

There are two limitations to the current study that should be considered when interpreting the results. First, this study did not identify the specific cell types that infiltrate the ADMs over time due to the lack of antibodies available for porcine tissue. However, previous studies have extensively characterized the recruitment/accumulation, proliferation, and differentiation of various stem/progenitor cells (e.g., perivascular stem cells, skeletal muscle myoblasts, $Sox2^+$ cells, and $CD133^+$ progenitor cells) to ECM scaffolds both *in vitro* and *in vivo*.[12,15,59–65] It is also known that host immune cells, especially macrophages, rapidly infiltrate and subsequently facilitate the degradation of ECM scaffolds.[66] Interestingly, ECM scaffold materials have been shown to modulate the macrophage phenotype toward regulatory M2 macrophages and that this directed macrophage polarization is a necessary and determinant factor of ECM scaffold-mediated constructive remodeling.[13,43] It is likely that some or all of the aforementioned cell populations are participating in the observed *in vivo* remodeling responses reported in this study, and future studies are needed to more fully characterize the cellular response to each material in this application. Second, this study did not attempt to characterize the mechanical properties of the ADMs/remodeled tissues over time. Rather, ADM degradation/remodeling was assessed using a commonly used qualitative histomorphologic scoring system, which enabled quantitative comparison of materials both over time and as a function of location within the explant. Further work is needed to more fully characterize the mechanical properties of each material for this clinical application.

Conclusion

The present study provides a quantitative spatial and temporal comparison of the *in vivo* responses to two commonly used ADMs in a large animal model of tissue expander breast reconstruction. Although both products are derived from cadaveric dermis, they were found to have different biochemical compositions and elicit distinct host tissue responses. This study provides an experimental platform for evaluating the host response to various types of biologic grafts such as ADMs that might be used in tissue expander breast reconstruction.

Acknowledgments

Partial funding for this study was provided by C. R. Bard, Inc. C.A.C. was partially supported by the National Science Foundation (NSF) Graduate Research Fellowship. The authors would also like to thank Tori Bain, Bernard Siu, and Brian Sicari for their contributions to data collection.

Disclosure Statement

This study was funded by C. R. Bard, Inc. (Davol), Warwick, Rhode Island. Ms. Gagne, Dr. Crapo, Dr. Badhwar, and Dr. Scott are employees of C. R. Bard. Dr. Garcia is a consultant, speaker, and research advisor/participant for C. R. Bard and for Sound Surgical Technologies, and a research advisor/participant for Mentor Corp. and Excaliard Pharmaceutical.

References

1. American Society of Plastic Surgeons, 2012 Plastic Surgery Statistics Report. 2012.
2. Spear, S.L., Parikh, P.M., Reisin, E., and Menon, N.G. Acellular dermis-assisted breast reconstruction. Aesthetic Plast Surg **32,** 418, 2008.

3. Breuing, K.H., and Colwell, A.S. Inferolateral AlloDerm hammock for implant coverage in breast reconstruction. Ann Plast Surg **59,** 250, 2007.
4. Namnoum, J.D. Expander/implant reconstruction with AlloDerm: recent experience. Plast Reconstr Surg **124,** 387, 2009.
5. Bindingnavele, V., Gaon, M., Ota, K.S., Kulber, D.A., and Lee, D.J. Use of acellular cadaveric dermis and tissue expansion in postmastectomy breast reconstruction. J Plast Reconstr Aesthet Surg **60,** 1214, 2007.
6. Breuing, K.H., and Warren, S.M. Immediate bilateral breast reconstruction with implants and inferolateral AlloDerm slings. Ann Plast Surg **55,** 232, 2005.
7. Nahabedian, M.Y. Acellular dermal matrices in primary breast reconstruction: principles, concepts, and indications. Plast Reconstr Surg **130,** 2012.
8. Vorotnikova, E., McIntosh, D., Dewilde, A., Zhang, J., Reing, J.E., Zhang, L., *et al.* Extracellular matrix-derived products modulate endothelial and progenitor cell migration and proliferation *in vitro* and stimulate regenerative healing *in vivo*. Matrix Biol **29,** 690, 2010.
9. Xu, R., Boudreau, A., and Bissell, M.J. Tissue architecture and function: dynamic reciprocity via extra- and intracellular matrices. Cancer Metastasis Rev **28,** 167, 2009.
10. Nelson, C.M., and Bissell, M.J. Of extracellular matrix, scaffolds, and signaling: tissue architecture regulates development, homeostasis, and cancer. Annu Rev Cell Dev Biol **22,** 287, 2006.
11. Beattie, A.J., Gilbert, T.W., Guyot, J.P., Yates, A.J., and Badylak, S.F. Chemoattraction of progenitor cells by remodeling extracellular matrix scaffolds. Tissue Eng Part A **15,** 1119, 2009.
12. Reing, J.E., Zhang, L., Myers-Irvin, J., Cordero, K.E., Freytes, D.O., Heber-Katz, E., *et al.* Degradation products of extracellular matrix affect cell migration and proliferation. Tissue Eng Part A **15,** 605, 2009.
13. Brown, B.N., Valentin, J.E., Stewart-Akers, A.M., McCabe, G.P., and Badylak, S.F. Macrophage phenotype and remodeling outcomes in response to biologic scaffolds with and without a cellular component. Biomaterials **30,** 1482, 2009.
14. Crapo, P.M., Gilbert, T.W., and Badylak, S.F. An overview of tissue and whole organ decellularization processes. Biomaterials **32,** 3233, 2011.
15. Turner, N.J., Yates, A.J., Jr., Weber, D.J., Qureshi, I.R., Stolz, D.B., Gilbert, T.W., *et al.* Xenogeneic extracellular matrix as an inductive scaffold for regeneration of a functioning musculotendinous junction. Tissue Eng Part A **16,** 3309, 2010.
16. Grauss, R.W., Hazekamp, M.G., Oppenhuizen, F., van Munsteren, C.J., Gittenberger-de Groot, A.C., and DeRuiter, M.C. Histological evaluation of decellularised porcine aortic valves: matrix changes due to different decellularisation methods. Eur J Cardiothorac Surg **27,** 566, 2005.
17. Dahl, S.L., Koh, J., Prabhakar, V., and Niklason, L.E. Decellularized native and engineered arterial scaffolds for transplantation. Cell Transplant **12,** 659, 2003.
18. Chen, R.N., Ho, H.O., Tsai, Y.T., and Sheu, M.T. Process development of an acellular dermal matrix (ADM) for biomedical applications. Biomaterials **25,** 2679, 2004.
19. Cartmell, J.S., and Dunn, M.G. Effect of chemical treatments on tendon cellularity and mechanical properties. J Biomed Mater Res **49,** 134, 2000.
20. Kropp, B.P., Eppley, B.L., Prevel, C.D., Rippy, M.K., Harruff, R.C., Badylak, S.F., *et al.* Experimental assessment of small intestinal submucosa as a bladder wall substitute. Urology **46,** 396, 1995.
21. Uygun, B.E., Soto-Gutierrez, A., Yagi, H., Izamis, M.L., Guzzardi, M.A., Shulman, C., *et al.* Organ reengineering through development of a transplantable recellularized liver graft using decellularized liver matrix. Nat Med **16,** 814, 2010.
22. Petersen, T.H., Calle, E.A., Zhao, L., Lee, E.J., Gui, L., Raredon, M.B., *et al.* Tissue-engineered lungs for *in vivo* implantation. Science **329,** 538, 2010.
23. Ott, H.C., Clippinger, B., Conrad, C., Schuetz, C., Pomerantseva, I., Ikonomou, L., *et al.* Regeneration and orthotopic transplantation of a bioartificial lung. Nat Med **16,** 927, 2010.
24. Karabekmez, F.E., Duymaz, A., and Moran, S.L. Early clinical outcomes with the use of decellularized nerve allograft for repair of sensory defects within the hand. Hand **4,** 245, 2009.
25. Flynn, L.E. The use of decellularized adipose tissue to provide an inductive microenvironment for the adipogenic differentiation of human adipose-derived stem cells. Biomaterials **31,** 4715, 2010.
26. Ott, H.C., Matthiesen, T.S., Goh, S.K., Black, L.D., Kren, S.M., Netoff, T.I., *et al.* Perfusion-decellularized matrix: using nature's platform to engineer a bioartificial heart. Nat Med **14,** 213, 2008.
27. Badylak, S.F. Xenogeneic extracellular matrix as a scaffold for tissue reconstruction. Transpl Immunol **12,** 367, 2004.
28. Chen, F., Yoo, J.J., and Atala, A. Acellular collagen matrix as a possible ''off the shelf'' biomaterial for urethral repair. Urology **54,** 407, 1999.
29. Dellgren, G., Eriksson, M., Brodin, L.A., and Radegran, K. The extended Biocor stentless aortic bioprosthesis. Early clinical experience. Scand Cardiovasc J **33,** 259, 1999.
30. Harper, C. Permacol: clinical experience with a new biomaterial. Hosp Med **62,** 90, 2001.
31. Kolker, A.R., Brown, D.J., Redstone, J.S., Scarpinato, V.M., and Wallack, M.K. Multilayer reconstruction of abdominal wall defects with acellular dermal allograft (AlloDerm) and component separation. Ann Plast Surg **55,** 36, 2005.
32. Lee, M.S. GraftJacket augmentation of chronic Achilles tendon ruptures. Orthopedics **27,** s151, 2004.
33. Metcalf, M.H., Savoie Iii, F.H., and Kellum, B. Surgical technique for xenograft (SIS) augmentation of rotator-cuff repairs. Oper Techn Orthop **12,** 204, 2002.
34. Wainwright, D.J. Use of an acellular allograft dermal matrix (AlloDerm) in the management of full-thickness burns. Burns **21,** 243, 1995.
35. Badylak, S.F., Freytes, D.O., and Gilbert, T.W. Extracellular matrix as a biological scaffold material: structure and function. Acta Biomater **5,** 1, 2009.
36. Sellaro, T.L., Ravindra, A.K., Stolz, D.B., and Badylak, S.F. Maintenance of hepatic sinusoidal endothelial cell phenotype *in vitro* using organ-specific extracellular matrix scaffolds. Tissue Eng **13,** 2301, 2007.
37. Lin, P., Chan, W.C., Badylak, S.F., and Bhatia, S.N. Assessing porcine liver-derived biomatrix for hepatic tissue engineering. Tissue Eng **10,** 1046, 2004.
38. Sellaro, T.L., Ranade, A., Faulk, D.M., McCabe, G.P., Dorko, K., Badylak, S.F., *et al.* Maintenance of human hepatocyte function *in vitro* by liver-derived extracellular matrix gels. Tissue Eng Part A **16,** 1075, 2010.
39. Wicha, M.S., Lowrie, G., Kohn, E., Bagavandoss, P., and Mahn, T. Extracellular matrix promotes mammary epithelial

growth and differentiation *in vitro*. Proc Natl Acad Sci U S A **79,** 3213, 1982.
40. Badylak, S.F., Valentin, J.E., Ravindra, A.K., McCabe, G.P., and Stewart-Akers, A.M. Macrophage phenotype as a determinant of biologic scaffold remodeling. Tissue Eng Part A **14,** 1835, 2008.
41. Keane, T.J., Londono, R., Turner, N.J., and Badylak, S.F. Consequences of ineffective decellularization of biologic scaffolds on the host response. Biomaterials **33,** 1771, 2012.
42. Valentin, J.E., Badylak, J.S., McCabe, G.P., and Badylak, S.F. Extracellular matrix bioscaffolds for orthopaedic applications. A comparative histologic study. J Bone Joint Surg Am **88,** 2673, 2006.
43. Brown, B.N., Londono, R., Tottey, S., Zhang, L., Kukla, K.A., Wolf, M.T., *et al.* Macrophage phenotype as a predictor of constructive remodeling following the implantation of biologically derived surgical mesh materials. Acta Biomater **8,** 978, 2012.
44. Freytes, D.O., Tullius, R.S., and Badylak, S.F. Effect of storage upon material properties of lyophilized porcine extracellular matrix derived from the urinary bladder. J Biomed Mater Res B Appl Biomater **78,** 327, 2006.
45. Reing, J.E., Brown, B.N., Daly, K.A., Freund, J.M., Gilbert, T.W., Hsiong, S.X., *et al.* The effects of processing methods upon mechanical and biologic properties of porcine dermal extracellular matrix scaffolds. Biomaterials **31,** 8626, 2010.
46. Faulk, D.M., Carruthers, C.A., Warner, H.J., Kramer, C.R., Reing, J.E., Zhang, L., *et al.* The effect of detergents on the basement membrane complex of a biologic scaffold material. Acta Biomater **10,** 183, 2014.
47. Garcia, O., Jr., and Scott, J.R. Analysis of acellular dermal matrix integration and revascularization following tissue expander breast reconstruction in a clinically relevant large-animal model. Plast Reconstr Surg **131,** 2013.
48. Valentin, J.E., Turner, N.J., Gilbert, T.W., and Badylak, S.F. Functional skeletal muscle formation with a biologic scaffold. Biomaterials **31,** 7475, 2010.
49. Mase, V.J., Jr., Hsu, J.R., Wolf, S.E., Wenke, J.C., Baer, D.G., Owens, J., *et al.* Clinical application of an acellular biologic scaffold for surgical repair of a large, traumatic quadriceps femoris muscle defect. Orthopedics **33,** 511, 2010.
50. Boruch, A.V., Nieponice, A., Qureshi, I.R., Gilbert, T.W., and Badylak, S.F. Constructive remodeling of biologic scaffolds is dependent on early exposure to physiologic bladder filling in a canine partial cystectomy model. J Surg Res **161,** 217, 2010.
51. Mantovani, F., Trinchieri, A., Castelnuovo, C., Romano, A.L., and Pisani, E. Reconstructive urethroplasty using porcine acellular matrix. Eur Urol **44,** 600, 2003.
52. Nieponice, A., McGrath, K., Qureshi, I., Beckman, E.J., Luketich, J.D., Gilbert, T.W., *et al.* An extracellular matrix scaffold for esophageal stricture prevention after circumferential EMR. Gastrointest Endosc **69,** 289, 2009.
53. Badylak, S., Meurling, S., Chen, M., Spievack, A., and Simmons-Byrd, A. Resorbable bioscaffold for esophageal repair in a dog model. J Pediatr Surg **35,** 1097, 2000.
54. Badylak, S.F., Hoppo, T., Nieponice, A., Gilbert, T.W., Davison, J.M., and Jobe, B.A. Esophageal preservation in five male patients after endoscopic inner-layer circumferential resection in the setting of superficial cancer: a regenerative medicine approach with a biologic scaffold. Tissue Eng Part A **17,** 1643, 2011.
55. Badylak, S.F., Kochupura, P.V., Cohen, I.S., Doronin, S.V., Saltman, A.E., Gilbert, T.W., *et al.* The use of extracellular matrix as an inductive scaffold for the partial replacement of functional myocardium. Cell Transplant **15 Suppl 1,** S29, 2006.
56. Akhyari, P., Aubin, H., Gwanmesia, P., Barth, M., Hoffmann, S., Huelsmann, J., *et al.* The quest for an optimized protocol for whole-heart decellularization: a comparison of three popular and a novel decellularization technique and their diverse effects on crucial extracellular matrix qualities. Tissue Eng Part C Methods **17,** 915, 2011.
57. Du, L., Wu, X., Pang, K., and Yang, Y. Histological evaluation and biomechanical characterisation of an acellular porcine cornea scaffold. Br J Ophthalmol **95,** 410, 2011.
58. Brown, B.N., Freund, J.M., Han, L., Rubin, J.P., Reing, J.E., Jeffries, E.M., *et al.* Comparison of three methods for the derivation of a biologic scaffold composed of adipose tissue extracellular matrix. Tissue Eng Part C Methods **17,** 411, 2011.
59. Agrawal, V., Siu, B.F., Chao, H., Hirschi, K.K., Raborn, E., Johnson, S.A., *et al.* Partial characterization of the Sox2+ cell population in an adult murine model of digit amputation. Tissue Eng Part A **18,** 1454, 2012.
60. Wolf, M.T., Daly, K.A., Reing, J.E., and Badylak, S.F. Biologic scaffold composed of skeletal muscle extracellular matrix. Biomaterials **33,** 2916, 2012.
61. Crisan, M., Yap, S., Casteilla, L., Chen, C.W., Corselli, M., Park, T.S., *et al.* A perivascular origin for mesenchymal stem cells in multiple human organs. Cell Stem Cell **3,** 301, 2008.
62. Agrawal, V., Johnson, S.A., Reing, J., Zhang, L., Tottey, S., Wang, G., *et al.* Epimorphic regeneration approach to tissue replacement in adult mammals. Proc Natl Acad Sci U S A **107,** 3351, 2010.
63. Tottey, S., Corselli, M., Jeffries, E.M., Londono, R., Peault, B., and Badylak, S.F. Extracellular matrix degradation products and low-oxygen conditions enhance the regenerative potential of perivascular stem cells. Tissue Eng Part A **17,** 37, 2011.
64. Tottey, S., Johnson, S.A., Crapo, P.M., Reing, J.E., Zhang, L., Jiang, H., *et al.* The effect of source animal age upon extracellular matrix scaffold properties. Biomaterials **32,** 128, 2011.
65. Turner, N.J., Johnson, S.A., and Badylak, S.F. A histomorphologic study of the normal healing response following digit amputation in C57bl/6 and MRL/MpJ mice. Arch Histol Cytol **73,** 103, 2010.
66. Valentin, J.E., Stewart-Akers, A.M., Gilbert, T.W., and Badylak, S.F. Macrophage participation in the degradation and remodeling of extracellular matrix scaffolds. Tissue Eng Part A **15,** 1687, 2009.

Address correspondence to:
Stephen F. Badylak, DVM, PhD, MD
McGowan Institute for Regenerative Medicine
University of Pittsburgh
450 Technology Drive
Suite 300
Pittsburgh, PA 15219

E-mail: badylaks@upmc.edu

Received: February 4, 2014
Accepted: June 13, 2014
Online Publication Date: September 26, 2014